

IL-4/CXCL12 loop is a key regulator of lymphoid stroma function in follicular lymphoma

Shubham Pandey, Frédéric Mourcin, Tony Marchand, Saba Nayar, Marion Guirriec, Céline Pangault, Céline Monvoisin, Patricia Amé-Thomas, Fabien Guilloton, Joelle Dulong, et al.

▶ **To cite this version:**

Shubham Pandey, Frédéric Mourcin, Tony Marchand, Saba Nayar, Marion Guirriec, et al.. IL-4/CXCL12 loop is a key regulator of lymphoid stroma function in follicular lymphoma. Blood, 2017, 129 (18), pp.2507-2518. 10.1182/blood-2016-08-737239 . hal-01555850

HAL Id: hal-01555850

https://univ-rennes.hal.science/hal-01555850

Submitted on 4 Jul 2017

HAL is a multi-disciplinary open access archive for the deposit and dissemination of scientific research documents, whether they are published or not. The documents may come from teaching and research institutions in France or abroad, or from public or private research centers.

L'archive ouverte pluridisciplinaire **HAL**, est destinée au dépôt et à la diffusion de documents scientifiques de niveau recherche, publiés ou non, émanant des établissements d'enseignement et de recherche français ou étrangers, des laboratoires publics ou privés.

IL-4/CXCL12 loop is a key regulator of lymphoid stroma function in follicular lymphoma

Shubham Pandey[1], Frédéric Mourcin[1], Tony Marchand[1,2], Saba Nayar[3], Marion Guirriec[1], Céline Pangault[1,4], Céline Monvoisin[1], Patricia Amé-Thomas[1,4], Fabien Guilloton[1], Joelle Dulong[1,4], Mark Coles[5], Thierry Fest[1,4], Anja Mottok[6], Francesca Barone[3] and Karin Tarte[1,4]

[1] UMR U917, INSERM, Université Rennes 1, EFS Bretagne, Equipe Labellisée Ligue Contre le Cancer, Rennes, France
[2] CHU de Rennes, Service d'Hématologie Clinique, Rennes, France
[3] UK Centre for Translational Inflammation Research, Institute of Inflammation and Ageing, College of Medical & Dental Sciences, University of Birmingham Research Laboratories, Queen Elizabeth Hospital, Birmingham, UK
[4] CHU de Rennes, Pôle de Biologie, Rennes, France
[5] Centre for Immunology and Infection, Department of Biology and Hull York Medical School, University of York, York, UK
[6] Centre for Lymphoid Cancer, British Columbia Cancer Agency and Department of Pathology and Laboratory Medicine, University of British Columbia, Vancouver, BC V5Z 1L3, Canada

Running title: CXCL12 regulation in lymphoma-infiltrating stroma

Scientific category: LYMPHOID NEOPLASIA

Correspondence
Karin Tarte, INSERM, UMR U917, Faculté de Médecine, 2 Avenue du Pr Léon Bernard, F-35043 Rennes; e-mail: karin.tarte@univ-rennes1.fr. Phone: +33 (0) 223 234 512, fax: +33 (0) 223 234 958

Abstract word count: 201
Article word count: 4558
Number of Figures: 6
Reference count: 61

KEY POINTS

1. FL-infiltrating stromal cells overexpress CXCL12 that triggers FL B-cell migration, adhesion, and activation

2. Polarization into CXCL12^{hi} stroma involves IL-4^{pos} T_{FH}, unlike TNF^{pos} malignant B cells, revealing an indirect protumoral activity of FL-T_{FH}

ABSTRACT

Follicular lymphoma (FL) is the most frequent indolent lymphoma and is characterized by the accumulation of germinal center-derived malignant B cells engaged in a bidirectional crosstalk with their supportive microenvironment in invaded lymph nodes (LN) and bone marrow (BM). T follicular helper cells (T_{FH}) and infiltrating stromal cells have been shown to favor FL B-cell growth but the mechanisms of their protumoral effect and how LN/BM microenvironment is converted into a lymphoma-permissive cell niche remain poorly understood. We demonstrated here that FL-infiltrating LN and BM stromal cells overexpressed CXCL12 *in situ*. IL-4^{hi} FL-T_{FH}, unlike FL B cells themselves, triggered CXCL12 upregulation in human stromal cell precursors. In agreement, expression of CXCL12 was associated with IL-4 expression and signaling within the FL BM and LN niches. This IL-4/CXCL12 axis was amplified in activated lymphoid stromal cells as shown in our *in vitro* model of human lymphoid stroma differentiation and in an inducible mouse model of ectopic lymphoid organ formation. Finally, CXCL12 triggered primary FL B-cell activation, migration, and adhesion, a process antagonized by Btk and PI3K inhibitors. These data identified the IL-4/CXCL12 loop as a previously unrecognized pathway involved in lymphoid stroma polarization and as a potential therapeutic target in FL patients.

INTRODUCTION

Tumors are now considered as a complex ecosystem in which the dynamic and mutualistic interactions between cancer cells and their surrounding microenvironment drive the coevolution of malignant cells and their supportive niche throughout the life history of the tumor[1]. Cancer-associated fibroblasts (CAFs) have been recently recognized as key players of cancer microenvironment with critical roles in tumor initiation, progression, metastatic dissemination, immune escape, and drug resistance. CAFs make up a highly heterogeneous population of activated reprogrammed myofibroblasts exhibiting specific phenotype, proliferation rate, gene expression profile, and epigenetic features[2]. They are supposedly derived from mesenchymal precursors, including mesenchymal stromal cells (MSCs), that could differentiate locally or are recruited from bone marrow (BM) or neighboring adipose tissue[3,4]. Whereas tumor cells contribute to the polarization of protumoral CAFs, infiltrating immune cells also shape the recruitment and activation of stromal cells inside tumors[5]. Myeloid cells were proposed as major drivers of stroma activation, but B and T cells could also modulate stroma functions. Such crosstalk has been well described in normal secondary lymphoid organs where adaptive immune cells are known to produce factors, in particular tumor necrosis factor alpha (TNF) and lymphotoxin $\alpha 1\beta 2$ (LT) that cooperate to support differentiation and maintenance of lymphoid stromal cells, including T-cell zone fibroblastic reticular cells (FRCs) and B-cell zone follicular dendritic cells (FDCs)[6-8]. Whereas CAFs could display some features of lymphoid stromal cells[9,10], the precise relationship between CAFs and lymphoid stroma is not well understood.

Follicular lymphoma (FL), the most frequent indolent lymphoma, is characterized by a long preclinical stage, a slow clinical course with multiple relapses, and a strong dependence on a specific microenvironment, including in particular $CD4^{pos}$ T cells and stromal cells[11,12]. FL-infiltrating T cells are enriched for activated T follicular helper cells (T_{FH}) able to sustain survival of malignant B cells *in vitro* and characterized by a specific cytokine profile[13,14]. T_{FH}-derived IL-4 has been shown to directly trigger FL B-cell activation as indicated by STAT6 phosphorylation[15], upregulation of surface IgM[16], and induction of CCL22 and CCL17 secretion[17]. Moreover, IL-4 could indirectly contribute to the polarization and organization of the FL protumoral cell niche. In particular, IL-4 is a well-known inducer of dendritic cell-

specific intercellular adhesion molecule-3-grabbing nonintegrin (DC-SIGN), a mannose-binding lectin recently implicated in the antigen-independent triggering of FL BCR by tumor-associated macrophages[16]. Whether IL-4 could modulate the properties of FL-infiltrating stromal cells has never been explored.

As expected for a malignancy resulting from the transformation of germinal center (GC)-derived B cells, FL-CAFs essentially display some features of lymphoid stromal cells[18]. Accordingly, the typical BM infiltration pattern of FL is characterized by a local enrichment of $CD4^{pos}$ T cells[19] and ectopic development of an heterogeneous population of lymphoid-like stromal cells[20,21]. This emphasizes the pivotal role of these two cell subsets in FL pathogenesis and a potential common stromal program in FL lymph nodes (LN) and BM. We previously demonstrated that MSCs obtained from FL-BM (FL-MSCs) exhibit a specific gene expression profile compared with MSCs from healthy donor BM (HD-MSCs) including an enrichment of a lymphoid stroma signature, associated with an increased capacity to sustain malignant B-cell growth[22]. In addition, FL-MSCs produce higher levels of both CCL2 and IL-8, whose secretion is upregulated in HD-MSCs by FL B cells[22,23]. These data indicate that a dynamic reciprocal cooperation program is activated between FL B cells and FL-infiltrating stromal cells and results in the formation of the lymphoma-permissive stromal cell niche. Little is known about how lymphoma B cells get access to and are retained within their tumor niches inside LN and BM but both CXCR4 and CCR7 have been involved in these processes[24,25].

Aiming at a better understanding of FL-stroma protumoral phenotype, we unraveled a specific upregulation of CXCL12 in both LN- and BM-infiltrating stromal cells. Moreover, we revealed that CXCL12 induction was not related to a crosstalk with TNF-producing malignant B-cells but with IL-4-producing FL-T_{FH}. Interestingly, such IL-4/CXCL12 loop was also efficient in activated lymphoid-like stromal cells both *in vitro* and *in vivo* and should be considered as a previously unrecognized pathway involved in lymphoid stroma polarization. Finally, the demonstration that CXCL12 favored malignant B-cell migration, adhesion, and activation argued for considering IL-4/ CXCL12 loop as a therapeutic target to disrupt FL protective cell niches.

PATIENTS, MATERIALS, AND METHODS

Human tissue and cell samples

Subjects were recruited under institutional review board approval following informed consent process according to the declaration of Helsinki and the French National Cancer Institute (INCa) ethic committee recommendations. Lipoaspiration was performed from adults undergoing abdominal dermolipectomy. Adipose-derived stromal cells (ADSCs) were obtained as previously described from the stromal vascular fraction, were maintained in *α*MEM medium supplemented with 10% FCS (HyClone), 1 ng/mL of bFGF (Cellgenix), penicillin, and streptomycin and were used between passages 1 and 3[26]. BM aspirates were obtained from FL patients and age-matched HD undergoing cardiac surgery, BM plasma was frozen, and HD- and FL-MSCs were obtained as previously described[22]. Tonsils were obtained from children undergoing routine tonsillectomy. LN and BM biopsies were also obtained from FL patients. Tonsil and FL B cells were purified using the B-cell isolation kit II (Miltenyi Biotec). FL-T_{FH} were sorted using a FACSAria (BD Biosciences) as described[13].

Immunohistofluorescence and Immunohistochemistry

Tonsils, FL-LN, and non-invaded/invaded FL-BM were embedded in OCT (Tissue-Tek OCT Compound). Tonsils and FL-LN sections where analyzed for CXCL12, podoplanin, and CD21 long isoform (CD21L) whereas BM sections were analyzed for CXCL12 and CD20 expression. Immunohistochemistry for pSTAT6 and CXCL12 was applied to a tissue microarray of 195 formalin-fixed, paraffin-embedded tissue specimens from 186 patients diagnosed with FL[27,28]. For details, see online Supplemental file.

Chemokine quantification

CXCL12 was quantified on culture supernatants of ADSCs treated or not with TNF/LT or IL-4 and BM plasma obtained from HD and FL patients by ELISA (R&D system).

Real time quantitative PCR

RNA extraction from human cell suspensions and mouse tissues was done using RNeasy Kit (Qiagen). Human tissue sections were homogeneized using QIAzol lysis

reagent RNA (Qiagen) and RNA was extracted by phenol/chloroform. cDNA was synthesized using Superscript II reverse transcriptase, followed by RT-QPCR. Assay-on-demand primers, probes, and TaqMan Universal Master Mix were obtained from Life Technologies. Gene expression was measured using StepOnePlus (Life Technologies) based on ΔCt calculation method. *CDKN1B*, *EIF2B1*, *PUM1* were determined as appropriate internal controls for ADSCs and *B2M*, *CASC3* for human LN and BM tissue samples, using TaqMan Endogenous Control Assays (Life Technologies). For mice samples, *Pdgfrβ* was used as an endogenous control. For each sample, the Ct value for the gene of interest was determined and normalized to its respective mean value of housekeeping genes.

Stromal cell stimulation

ADSCs were treated using TNF (20ng/mL)/LT (100ng/mL) or IL-4 (5ng/mL) (R&D Systems) for 3 days. When indicated, ADSCs were cultured in the presence of TNF/LT for 3 days and then cells were treated or not with IL-4 for 3 additional days. Purified FL-T_{FH} (10^5/mL) or FL B cells ($5x10^5$ cells/mL) were cocultured with confluent ADSCs for 48hrs before sorting of $CD45^{neg}CD105^{pos}DAPI^{neg}$ viable stromal cells and *CXCL12* quantification by RQ-PCR.

Immunofluorescence

ADSCs stimulated with TNF/LT or IL-4 for 3 days were analyzed as described previously[29]. In brief, cells were fixed in 2% PFA and stained with rat anti–podoplanin and mouse anti-transglutaminase (TGM2) antibodies (Abcam) followed by labeling with anti-rat Alexa 488 and anti-mouse Alexa 594 secondary antibodies (Jackson Immunoresearch). Coverslips were mounted with Mowiol including Sytox blue (Life Technologies) and examined using confocal microscope (SP5X, Leica Microsystem). Digital images were analyzed by ImageJ software.

Flow cytometry

Viable cells were analyzed after $DAPI^{pos}$ or $TOPRO\text{-}3^{pos}$ cell exclusion (Life Technologies) using following monoclonal antibodies (mAbs): FITC-conjugated anti-CD19 and anti-CD20, PE-conjugated anti-CD106/VCAM-1 and anti-CD54/ICAM-1 (Beckman Coulter), PC7-conjugated anti-CXCR4, and PC5.5-conjugated anti-podoplanin/gp38 (eBioscience). Appropriate isotype-matched mAbs were used to

obtain mean fluorescence intensity (MFI) ratios and analyses were performed using CyAn or Gallios (Beckman Coulter) flow cytometers.

Mice and salivary gland cannulation

Balb/c, *Il4-rαko and Il4ko* mice were bred and maintained under specific pathogen-free conditions in the Biomedical Service Unit at the University of Birmingham according to Home Office and local ethics committee regulations. The submandibular glands of female wild-type and knock-out mice (8-12 weeks old) were intraductally cannulated with 10^8-10^9 p.f.u. of luciferase-encoding replication-defective adenovirus (Ad5), as previously described[30]. Salivary glands were harvested at various time points post cannulation and used for evaluation of luciferase activity and quantification of gene expression.

Cell signaling

ADSCs were treated or not with TNF/LT for 24hrs, then starved for 2 hours in RPMI-1%FCS before stimulation with IL-4 (5ng/mL) for 5min. FL B cells were starved for 4 hours, treated or not for 30min by Ibrutinib (Selleckchem, 10μM), and stimulated by beads alone or CXCL12-Fc coated beads at 30μg/mL for 60min. Analysis of IL-4-driven and CXCL12-driven signaling was performed as detailed in the Supplemental Methods.

Migration and adhesion assays

Purified FL B cells were treated or not with Idelalisib/CAL101 (5μM, Cayman Chemicals), Ibrutinib (10μM) or AMD3100 (1μM, Sigma) for 30min and were used for migration and adhesion to CXCL12 as detailed in the Supplemental Methods.

Statistical analysis

Statistical analyses were performed using Prism software version 6 (GraphPad Software Inc) using the non-parametric Wilcoxon test for matched pairs or the Mann-Whitney nonparametric U test as appropriate. For association analysis between CXCL12 and pSTAT6 expression in human FL tissue biopsies we performed a Chi-square test.

RESULTS

CXCL12 is upregulated within FL stromal cell niches

To decipher the driving signaling involved in the recruitment and homing of malignant FL B cells to their supportive cell niche, and given the key role of CXCL12 in normal GC organization, we first decided to evaluate the expression of CXCL12 by tumor-infiltrating stromal cells. In chronically inflamed tonsils, CXCL12-expressing stromal cells formed a dense meshwork in perifollicular and interfollicular areas, consisting in podoplanin/gp38^{pos} fibroblastic reticular cells (FRC) (Figure 1A and S2). Inside tonsil GC, CXCL12 staining was always scarce and strictly restricted to CD21L^{neg} cells, whereas the CD21L^{pos} mature follicular dendritic cell (FDC) network was CXCL12-negative, as previously reported in mice[31]. Conversely, immunohistofluorescence analysis revealed that CXCL12 was overexpressed in stromal cells within follicles in 8/14 FL patients and *CXCL12* mRNA was significantly upregulated in FL LN compared to tonsil samples (Figure 1A-B and S3). Interestingly, CXCL12 overexpression was associated with a variable loss of the CD21L FDC marker as revealed by RQ-PCR and immunohistofluorescence experiments (Figure S3B).

We next decided to focus on the BM FL cell niche and performed immunohistofluorescence analysis on undecalcified biopsies from FL patients with and without BM involvement. In the absence of infiltrating malignant B cells, CXCL12 staining revealed a diffuse and homogeneous stromal cell network (Figure S4). BM sections from BM-invaded patients showed aggregates of CD20^{pos} FL B cells with preferential paratrabecular localization. These B-cell infiltrated areas displayed increased CXCL12 labeling compared to areas outside lymphoma infiltrates (Figure 1C). In agreement, CXCL12 quantification in BM plasma showed a 4-fold increased CXCL12 level in FL BM (median: 4628 pg/ml, range: 726-7968 pg/ml, n=20) compared to age-matched HD BM (median: 1192 pg/ml, range: 56-3796 pg/ml, n=20, P<0.0001) (Figure 1D). Moreover, FL BM cells demonstrated a higher expression of *CXCL12* compared to BM cells obtained from age-matched HD (Figure 1E). Finally we checked *CXCL12* level in FL-MSCs that have been proposed as a good *in vitro* model to study lymphoma-driven alterations of stromal microenvironment[22,23]. Interestingly, we revealed that FL-MSCs exhibited a significantly higher expression of *CXCL12* than HD-MSCs.

Altogether, these data argued for an upregulation of CXCL12 within FL stromal cell niches and raised the question of the mechanisms underlying this upregulation, including the factors involved and the inducer cell type.

IL-4, unlike TNF/LT, upregulates CXCL12 in stromal cells

We previously demonstrated that human BM-MSCs could acquire *in vitro* a lymphoid-like stroma phenotype, associated with an upregulation of CCL19, BAFF, CCL2 and IL-8, in response to TNF/LT stimulation[22,23,29]. We thus decided to evaluate first how TNF/LT modulated CXCL12 production by MSCs. For that purpose we developed a new *in vitro* model of lymphoid-stroma polarization based on adipose-derived MSCs (ADSCs) since adipose tissue has been identified as a precursor of lymphoid stroma for lymph nodes and other lymphoid structures[32]. Interestingly, human ADSCs, like BM-MSCs[29], were able to acquire a FRC-like phenotype upon stimulation with TNF/LT, including upregulation of ICAM-1/CD54, VCAM-1/CD106, gp38/podoplanin, BAFF, and CCL19, and construction of a dense extracellular meshwork of transglutaminase and podoplanin (Figure S5). In addition, ADSCs overexpressed *CCL2* and *IL8* in response to TNF/LT. In this validated model, we demonstrated a significant downregulation of CXCL12, at both mRNA and protein levels, in ADSCs stimulated by TNF/LT (Figure 2A).

IL-4 is the most strongly deregulated cytokine in FL[33] and is known to upregulate VCAM-1 on dermal fibroblasts[34]. We thus tested the impact of IL-4 stimulation on ADSCs. Interestingly, IL-4 strongly increased the expression of VCAM-1 but also the production of CXCL12 in mesenchymal precursors (Figure 2A-B). In addition, whereas TNF/LT decreased transglutaminase mRNA, IL-4 triggered both transglutaminase expression and redistribution at the surface of stromal cells (Figure 2B-C). Finally, IL-4 reduced podoplanin expression by ADSCs. As a whole, whereas TNF/LT promoted ADSC *in vitro* differentiation into VCAM-1^{pos}podoplanin^{hi}CXCL12^{lo} cells, IL-4 favored a VCAM-1^{hi}podoplanin^{lo}CXCL12^{hi} phenotype, and both TNF/LT and IL-4 induced the construction of an extracellular transglutaminase^{pos} meshwork. FL-T_{FH} were proposed as the major IL-4-producing cells within the FL cell niche[14] whereas malignant B cells produce no IL-4 but variably secrete TNF, previously involved in the induction of both CCL2 and IL-8 production by BM-MSCs[22,23]. In agreement, co-culture of stromal cells with TNF^{hi} malignant B cells induced a

decrease in CXCL12 expression. Conversely, purified $CD4^{pos}CXCR5^{hi}PD\text{-}1^{hi}$ FL-T_{FH} triggered an upregulation of CXCL12 in ADSCs (Figure 2D-E).

To further increase the relevance of these *in vitro* observations for FL biology, we evaluated the expression of IL-4 *in situ* in FL LN and BM. *IL4* mRNA was significantly upregulated in both FL cell niches (Figure 3A-B), unlike the IL-4-related cytokine *IL13* (Figure S6). In agreement, we revealed by Gene Set Enrichment Analysis (GSEA) approach, the enrichment for an IL-4 gene signature in sorted FL B cells compared to normal $CD19^{pos}IgD^{neg}CD38^{hi}CD10^{pos}CXCR4^{neg}$ tonsil centrocytes, thus confirming the activation of IL-4 signaling in FL (Figure S7). Since quantification of IL-4-producing cells *in vivo* is virtually impossible apart from IL-4 reporter mice, we examined STAT6 phosphorylation together with CXCL12 staining across a large series of FL LN samples, as previously described[27] (Figure 3C). We scored a sample as CXCL12 positive when CXCL12 expression within FL follicles was higher than in reactive GC used as on-slide controls. We then examined STAT6 phosphorylation in CXCL12 positive (n=32) *versus* CXCL12 negative (n=163) tumors. We observed a significant increase in STAT6 phosphorylation in the CXCL12 positive FL (P=0.013, Figure 3D). Moreover, *IL4* and *CXCL12* expression were positively correlated across 20 FL BM samples (Figure 3E) thus further confirming the relationship between IL-4 and CXCL12 within FL cell niches. Interestingly, within FL LN, transglutaminase was upregulated and podoplanin downregulated (Figure S6), thus mimicking the phenotype of IL-4-treated stromal cells. Collectively, these results suggest that an IL-4/CXCL12 loop is activated within FL cell niches and that IL-4 contributes to the phenotype of FL stroma.

Lymphoid stroma commitment is associated with an increased IL-4-dependent CXCL12 production

Having demonstrated that IL-4 could trigger CXCL12 expression by mesenchymal precursors, we decided to investigate its capacity to affect the production of CXCL12 by differentiated lymphoid stromal cells, thus mimicking the FL cell niche context. For that purpose, ADSCs previously committed to lymphoid stroma differentiation *in vitro* by priming with TNF/LT were treated by IL-4. As previously reported for resting stromal cells, FRC-like stromal cells upregulated CXCL12 in response to IL-4 at both mRNA and protein levels, whereas the TNF/LT combination retained its potential to decrease CXCL12 expression (Figure 4A). Strikingly, committed stromal cells could

produce significantly higher levels of CXCL12 than their resting counterpart after stimulation by IL-4. Of note, the same results were obtained for transglutaminase and VCAM-1; both induced more efficiently on lymphoid-like cells than on ADSCs by exogenous IL-4 (Figure 4B). We next explored the mechanism of this increased sensitivity of lymphoid stroma to IL-4 signaling. IL-4 induced STAT6 phosphorylation in resting stromal cells but TNF/LT-pretreated stromal cells exhibited a significantly stronger STAT6 phosphorylation in response to IL-4, as shown by both flow cytometry and western blot (Figure 4C).

In order to investigate *in vivo* the relevance of this IL-4/CXCL12 loop in regulating lymphoid stroma function we took advantage of an inducible mouse model of ectopic lymphoid organ formation, associated with a significant increase of lymphoid chemokine expression, induced by cannulation of murine salivary glands with a replication-deficient adenovirus[30]. In WT mice, *Il4* was strongly upregulated upon infection in cannulated glands with a peak at day 8 (Figure 5A). In parallel, *Cxcl12* expression was significantly increased within salivary glands (Figure 5B). Interestingly, moving our analysis to *Il4*$^{-/-}$ and *Il4r*$^{-/-}$ mice revealed that a blockade of IL-4 signaling pathway impaired CXCL12 expression from day 8 post-cannulation. Taken together, these findings confirm a role of IL-4 in the induction of CXCL12 in inflammatory non-malignant lymphoid organs, phenocopying the observation in human FL samples.

CXCL12 mediates FL B-cell activation

BCR activation is instrumenta

B-cell malignancies, leading to the recent development of therapeutic BCR inhibitors. Chemokine receptor signaling also involved various components of the BCR signaling pathways and both BTK and phosphoinositide 3'-kinase isoform p110δ (PI3Kδ) inhibitors were shown to abrogate tumor cell migration toward stromal cell-derived CXCL12 in chronic lymphocytic leukemia (CLL)[35,36]. Whereas we recently pointed up the efficacy of the BTK inhibitor Ibrutinib to abolish the crosstalk between FL B cells and tumor-associated macrophages[16], no study has been designed to decipher how Ibrutinib or the PI3Kδ inhibitor Idelalisib could affect stroma/FL B cell interactions. We first evaluated CXCR4 expression in FL. Interestingly, whereas purified FL B cells expressed significantly higher amount of *CXCR4* mRNA than their

normal centrocyte counterpart (Figure S8A), their membrane expression of CXCR4 was highly variable, as could be expected given the huge amount of CXCL12 within FL cell niche and the well-known ligand-dependent internalization of CXCR4 (data not shown). In agreement, as recently suggested[37], CXCR4 was re-expressed after a 4-hour *in vitro* culture in the absence of CXCL12, a process that did not alter FL B-cell survival (Figure S8B). We then evaluated primary FL B-cell migration in response to CXCL12 after *in vitro* starvation and demonstrated that it was similarly reduced in response to the CXCR4 inhibitor AMD3100, Ibrutinib, and Idelalisib (Figure 6A). Interestingly, CXCL12 expression was also mandatory to trigger FL B-cell adhesion to stromal cells, as shown by blocking experiments based on the use of CXCL12-Fc chimeric molecule or AMD3100 (Figure 6B). Moreover, same results were obtained using CXCL12 siRNA previously validated for their capacity to inhibit CXCL12 production by stromal cells (Figure 6B and S9). CXCL12 was described as an activator of SYK, another key mediator of BCR signaling, and its downstream targets, including ERK, in CLL B cells[38]. We demonstrated here that FL B cells could also respond to CXCR4 triggering by SYK and ERK phosphorylation (Figure 6C). Moreover, Ibrutinib was able to inhibit CXCL12-dependent ERK activation in primary FL B cells (Figure 6D). Of note, Ibrutinib decreased slightly but significantly the expression of CXCR4 on primary FL B cells (Figure S8C).

DISCUSSION

FL is a paradigm of microenvironment-dependent neoplasia and infiltrating stromal cells have been proposed as key organizers of FL cell niches[18]. However, specific features of FL CAFs *in situ* are relatively unexplored. A major emerging issue is thus to characterize FL stroma, looking for deregulation of tumor-supporting factors, to highlight the cellular and molecular determinants regulating this FL-specific stroma phenotype, and to evaluate the potential therapeutic impact of targeting the crosstalk between malignant B cells and their stromal cell niche.

Our study revealed that FL stromal cells variably but substantially upregulated CXCL12, the homeostatic chemokine supporting normal GC polarization into dark zone (DZ) and light zone (LZ)[39]. Of note, immunohistochemistry studies highlighted a lower percentage of FL samples harboring CXCL12^{hi} follicular stromal cells than immunohistofluorescence, but *CXCL12* mRNA was found upregulated in the majority of FL patients, suggesting that CXCL12 deregulation is a recurrent feature in FL. Given the major role of normal GC B-cell shuttling between DZ and LZ for their expansion, selection, and differentiation, CXCL12 is considered as a critical regulator of GC responses and its expression by lymphoid stromal cells is finely controlled. An intriguing question is thus to identify the origin of CXCL12^{hi} stromal cells within FL LN follicles. We confirmed here the disappearance of mature gp38^{hi}CD21L^{pos} FDCs in FL patients, a quite intriguing observation for a disease targeting centrocytes. Since FDCs are supposed to be sessile and long-lived cells, this loss of FDC markers in FL follicles has been initially proposed to result from local FDC dedifferentiation[40]. However, recent results revealed that the FDC network is more dynamic than previously anticipated with a burst of FDC differentiation from highly proliferating progenitors in inflammatory context [41]. These data suggest that LZ FDCs could be replaced in FL patients by new stromal cells. A first hypothesis is that CXCL12^{hi} FL stromal cells arise from the so-called CXCL12-expressing reticular cells (CRCs) recently identified among gp38^{pos}CD21/35^{neg} stromal cells of the GC DZ in mice[42]. CRCs lack the main FRC and FDC markers and were thus proposed as a distinct cell type even if they share a lineage precursor with both FRCs and FDCs[31]. Apart from CRCs, mouse FRCs also express CXCL12 and CRC and FRC networks are tightly connected. Moreover, a subset of FRCs localized in follicular regions has been very recently shown to contribute to B-cell homeostasis through the production of BAFF[43].

Interestingly, we pinpointed that gp38^{pos}CD21L^{neg} FRC network was dense and activated in FL patients. Whether CRCs or follicular FRCs could be considered as precursors of CXCL12^{hi} FL stroma remains to be determined. Interestingly, FRC activation and expansion have been proposed to rely on the delivery of LTβR signals by incoming naïve B and T cells in response to inflammatory stimuli[44] and expression of LT by normal GC B cells is mandatory for mature FDC differentiation[45]. Conversely, DZ CRCs do not require LT and TNF for maintenance of CXCL12 expression and network morphology[31]. In agreement, purified FL B cells exhibit a downregulation of *LTA* and *LTB* compared to normal GC B cells (Figure S10), thus providing an argument in favor of a CRC-like origin for FL stromal cells. The origin of CXCL12^{hi} FL stroma in invaded BM is even more puzzling. Within mouse BM, a subset of mesenchymal progenitors is characterized by a strong expression of CXCL12 and has been described in close contact with hematopoietic stem cells, B-cell progenitors, and long-lived plasma cells[46,47]. We reported here for the first time an upregulation of CXCL12 by human stromal cells admixed with ectopic malignant GC B cells. Unfortunately, the lack of relevant FL mouse model precludes cell tracking-based identification of FL stroma precursor cells.

Several mechanisms could cooperate in the modification of FL stromal cells and we previously demonstrated that malignant B cells directly trigger upregulation of stromal CCL2 in a TNF-dependent manner[22]. Interestingly, mouse B cells respond to the IL-4 burst associated with intestinal helminth infection by an increase in their expression of LT, which then interacts with LTβR^{pos} FRCs to induce their expansion and reorganization[48]. However, such process is unlikely to take place in FL, given the downregulation of LT on malignant B cells. In agreement, we revealed that primary FL B cells were not able to stimulate *in vitro* CXCL12 production in stromal cells, whereas FL-T_{FH} were efficient CXCL12-inducers. Several T cell-derived cytokines could favor CXCL12 expression by lymphoid stromal cells. In particular IL-22 could upregulate CXCL13 and CXCL12 in tertiary lymphoid organs thus favoring B-cell recruitment and autoantibody production[49]. In addition, IL-17 drives the differentiation of IL17Rc^{pos} pulmonary stromal cells from bronchus-associated lymphoid tissues into gp38^{pos}CD21/35^{neg}CXCL12^{pos} follicular stromal cells allowing GC formation in the absence of both FDC and LT^{pos} B cells[50]. Altogether these data suggest that infiltrating T cells producing Th17-associated cytokines could contribute to the polarization of cancer-infiltrating stromal cells. Within FL cell niche, malignant B cells

skew the Treg/Th17 balance in favor of intratumoral Treg[51] and FL-T_{FH} poorly express Th17-related markers, including *IL-17*, *IL-26,* and *RORC*[13,14]. IL-17 is thus probably not implicated in the differentiation of FL specific stroma. Conversely, given the association between CXCL12 expression and IL-4 expression/signaling within FL cell niches, it was tempting to speculate that IL-4, the main FL-T_{FH}-derived cytokine, could contribute to the stimulation of CXCL12 production by stromal cells. In agreement, we revealed for the first time that IL-4 could directly act on human mesenchymal progenitors and FRC-like cells to upregulate CXCL12, in the absence of LT-expressing B cells. Interestingly, IL-4 also triggered *in vitro* transglutaminase upregulation and gp38/podoplanin downregulation on stromal cells, a phenotype close to that identified *in situ* within FL cell niche, and upregulated CD106, that was previously reported to rescue lymphoma B cells from Rituximab-induced apoptosis[52]. IL-4 exerts thus a wide effect on tumor-supportive FL stromal cells. The source of IL-4 within FL BM remains unknown but even if their number is reduced compared to LN niche, PD-1^{pos} T cells could be detected in FL BM together with an increase of the CD4/CD8 T cell ratio and these T_{FH}/T_{FH}-like cells are likely to be involved[19,53]. In addition, IL-4 is also involved in the polarization of FL-infiltrating macrophages[16]. Altogether, these results highlight IL-4 as a key mediator and of FL pathogenesis and T_{FH}-stroma crosstalk as a new B-cell extrinsic mechanism supporting FL cell growth (Figure S11).

Whereas IL-4 and TNF/LT similarly induced some FRC-like features in MSCs, they exerted an antagonistic activity on CXCL12 and gp38/podoplanin expression, raising the question of the underlying signaling pathways. Interestingly, CXCL13 is also regulated in an opposite way by TNF and IL-4 in monocytes and macrophages even if, in this case, TNF acts as an inducer and IL-4 as a repressor[54]. In addition, TNF-induced classical NF-κB signaling was already shown to inhibit CXCL12 expression in human umbilical vein endothelial cells[55,56] and in a BM stromal cell line[52,53]. The demonstration that TNF/LT-primed stromal cells became more sensitive to IL-4-dependent CXCL12 upregulation, at least in part through an increased expression of STAT6 signaling molecule, deserves further investigations.

Besides their capacity to produce CXCL12, FL stromal cells have been proposed to contribute directly to FL B-cell growth through the expression of CD106, hedgehog family proteins, or BAFF, and indirectly through the recruitment of other components of the supportive FL cell niche, including tumor-associated macrophages and tumor-

associated neutrophils[18,22,23]. In agreement, targeting the crosstalk between malignant B cells and stromal cells is a promising therapeutic strategy. Among the possible approaches, the use of the BTK inhibitor Ibrutinib or the PI3Kδ inhibitor Idelalisib to impair CXCR4 signaling has been recently proposed in CLL[36,57] and we demonstrated here its relevance in FL. Other CXCR4 antagonists[58] as well as SYK inhibitors[38] are under evaluation for their capacity to counteract CXCL12 activity in B-cell malignancies and yielded interesting *in vitro* results. Targeting CXCL12 specifically produced by a subset of pancreatic cancer CAFs is sufficient to override tumor immunosuppression *in vivo* and reveals the antitumor effects of anti-PD-L1 immunotherapy[59]. This finding may have important clinical relevance in FL where immune-checkpoint blockade emerges as a valuable therapeutic approach. Finally, the use of JAK3 or STAT6 inhibitors, recently tested on CLL B cells[60], may override the effect of IL-4 on the induction of CXCL12 expression by stromal cells, but also on the activation of malignant B cells, in particular in combination with inhibition of BCR signaling pathway[61], and would be thus of potential relevance in FL patients.

ACKNOWLEDGMENTS

This work was supported by research grants from the Ligue Nationale Contre le Cancer (Equipe Labellisée and "Carte d'identité des Tumeurs" program) and the Institut National du cancer (INCA AAP PLBIO-14-40). SP was recipient of a doctoral fellowship from the FP7 Marie Curie Initial Training Network (ITN 289720 Stroma) and the Ligue Nationale Contre le Cancer. AM is supported by fellowship awards from the Mildred-Scheel-Cancer Foundation, the Michael Smith Foundation for Health Research and Lymphoma Canada. Immunofluorescence study was performed on the Microscopy Rennes Imaging Center (MRic-ALMF; UMS 6480 Biosit, Rennes, France). The authors are indebted to the Centre de Ressources Biologiques (CRB)-Santé (BB-0033-00056, http://www.crbsante-rennes.com) of Rennes hospital for its support in the processing of biological samples, Christophe Ruaux for providing tonsil samples, Erwan Flecher for providing normal bone marrow samples, and Nicolas Bertheuil for providing adipose tissues.

AUTHORSHIP CONTRIBUTIONS

SP: designed and performed experiments, analyzed data, and contributed writing; FM: designed and analyzed data, and contributed writing; TM, SB, MG, CP, CM, PAT, FG, JD: performed experiments and analyzed data; TF: provided samples; AM: performed immunohistochemical studies; MC, FB: designed and coordinated mouse study; KT: designed and supervised research, analyzed data, and wrote the paper.

CONFLICT-OF-INTEREST DISCLOSURE

The authors declare no competing financial interest.

REFERENCES

1. Hanahan D, Weinberg RA. Hallmarks of cancer: the next generation. *Cell*. 2011;144(5):646-674.
2. Ohlund D, Elyada E, Tuveson D. Fibroblast heterogeneity in the cancer wound. *J Exp Med*. 2014;211(8):1503-1523.
3. Cirri P, Chiarugi P. Cancer associated fibroblasts: the dark side of the coin. *Am J Cancer Res*. 2011;1(4):482-497.
4. Kidd S, Spaeth E, Watson K, et al. Origins of the tumor microenvironment: quantitative assessment of adipose-derived and bone marrow-derived stroma. *PLoS One*. 2012;7(2):e30563.
5. Turley SJ, Cremasco V, Astarita JL. Immunological hallmarks of stromal cells in the tumour microenvironment. *Nat Rev Immunol*. 2015;15(11):669-682.
6. Roozendaal R, Mebius RE. Stromal cell-immune cell interactions. *Annu Rev Immunol*. 2011;29:23-43.
7. Aguzzi A, Kranich J, Krautler NJ. Follicular dendritic cells: origin, phenotype, and function in health and disease. *Trends Immunol*. 2014;35(3):105-113.
8. Fletcher AL, Acton SE, Knoblich K. Lymph node fibroblastic reticular cells in health and disease. *Nat Rev Immunol*. 2015;15(6):350-361.
9. Shields JD, Kourtis IC, Tomei AA, Roberts JM, Swartz MA. Induction of lymphoidlike stroma and immune escape by tumors that express the chemokine CCL21. *Science*. 2010;328(5979):749-752.
10. Peduto L, Dulauroy S, Lochner M, et al. Inflammation recapitulates the ontogeny of lymphoid stromal cells. *J Immunol*. 2009;182(9):5789-5799.
11. Kridel R, Sehn LH, Gascoyne RD. Pathogenesis of follicular lymphoma. *J Clin Invest*. 2012;122(10):3424-3431.
12. Ame-Thomas P, Tarte K. The yin and the yang of follicular lymphoma cell niches: role of microenvironment heterogeneity and plasticity. *Semin Cancer Biol*. 2014;24:23-32.
13. Ame-Thomas P, Le Priol J, Yssel H, et al. Characterization of intratumoral follicular helper T cells in follicular lymphoma: role in the survival of malignant B cells. *Leukemia*. 2012;26(5):1053-1063.
14. Ame-Thomas P, Hoeller S, Artchounin C, et al. CD10 delineates a subset of human IL-4 producing follicular helper T cells involved in the survival of follicular lymphoma B cells. *Blood*. 2015;125(15):2381-2385.
15. Pangault C, Ame-Thomas P, Ruminy P, et al. Follicular lymphoma cell niche: identification of a preeminent IL-4-dependent T(FH)-B cell axis. *Leukemia*. 2010;24(12):2080-2089.
16. Amin R, Mourcin F, Uhel F, et al. DC-SIGN-expressing macrophages trigger activation of mannosylated IgM B-cell receptor in follicular lymphoma. *Blood*. 2015;126(16):1911-1920.
17. Rawal S, Chu F, Zhang M, et al. Cross talk between follicular Th cells and tumor cells in human follicular lymphoma promotes immune evasion in the tumor microenvironment. *J Immunol*. 2013;190(12):6681-6693.
18. Mourcin F, Pangault C, Amin-Ali R, Ame-Thomas P, Tarte K. Stromal cell contribution to human follicular lymphoma pathogenesis. *Front Immunol*. 2012;3:280.
19. Wahlin BE, Sander B, Christensson B, et al. Entourage: the immune microenvironment following follicular lymphoma. *Blood Cancer J*. 2012;2(1):e52.

20. Sangaletti S, Tripodo C, Portararo P, et al. Stromal niche communalities underscore the contribution of the matricellular protein SPARC to B-cell development and lymphoid malignancies. *Oncoimmunology*. 2014;3:e28989.
21. Vega F, Medeiros LJ, Lang WH, Mansoor A, Bueso-Ramos C, Jones D. The stromal composition of malignant lymphoid aggregates in bone marrow: variations in architecture and phenotype in different B-cell tumours. *Br J Haematol*. 2002;117(3):569-576.
22. Guilloton F, Caron G, Menard C, et al. Mesenchymal stromal cells orchestrate follicular lymphoma cell niche through the CCL2-dependent recruitment and polarization of monocytes. *Blood*. 2012;119(11):2556-2567.
23. Gregoire M, Guilloton F, Pangault C, et al. Neutrophils trigger a NF-kappaB dependent polarization of tumor-supportive stromal cells in germinal center B-cell lymphomas. *Oncotarget*. 2015;6(18):16471-16487.
24. Corcione A, Ottonello L, Tortolina G, et al. Stromal cell-derived factor-1 as a chemoattractant for follicular center lymphoma B cells. *J Natl Cancer Inst*. 2000;92(8):628-635.
25. Rehm A, Mensen A, Schradi K, et al. Cooperative function of CCR7 and lymphotoxin in the formation of a lymphoma-permissive niche within murine secondary lymphoid organs. *Blood*. 2011;118(4):1020-1033.
26. Bigot N, Mouche A, Preti M, et al. Hypoxia Differentially Modulates the Genomic Stability of Clinical-Grade ADSCs and BM-MSCs in Long-Term Culture. *Stem Cells*. 2015;33(12):3608-3620.
27. Boice M, Salloum D, Mourcin F, et al. Loss of the HVEM Tumor Suppressor in Lymphoma and Restoration by Modified CAR-T Cells. *Cell*. 2016;167(2):405-418 e413.
28. Kridel R, Xerri L, Gelas-Dore B, et al. The Prognostic Impact of CD163-Positive Macrophages in Follicular Lymphoma: A Study from the BC Cancer Agency and the Lymphoma Study Association. *Clin Cancer Res*. 2015;21(15):3428-3435.
29. Ame-Thomas P, Maby-El Hajjami H, Monvoisin C, et al. Human mesenchymal stem cells isolated from bone marrow and lymphoid organs support tumor B-cell growth: role of stromal cells in follicular lymphoma pathogenesis. *Blood*. 2007;109(2):693-702.
30. Bombardieri M, Barone F, Lucchesi D, et al. Inducible tertiary lymphoid structures, autoimmunity, and exocrine dysfunction in a novel model of salivary gland inflammation in C57BL/6 mice. *J Immunol*. 2012;189(7):3767-3776.
31. Rodda LB, Bannard O, Ludewig B, Nagasawa T, Cyster JG. Phenotypic and Morphological Properties of Germinal Center Dark Zone Cxcl12-Expressing Reticular Cells. *J Immunol*. 2015;195(10):4781-4791.
32. Benezech C, Mader E, Desanti G, et al. Lymphotoxin-beta receptor signaling through NF-kappaB2-RelB pathway reprograms adipocyte precursors as lymph node stromal cells. *Immunity*. 2012;37(4):721-734.
33. Calvo KR, Dabir B, Kovach A, et al. IL-4 protein expression and basal activation of Erk in vivo in follicular lymphoma. *Blood*. 2008;112(9):3818-3826.
34. Burger JA, Zvaifler NJ, Tsukada N, Firestein GS, Kipps TJ. Fibroblast-like synoviocytes support B-cell pseudoemperipolesis via a stromal cell-derived factor-1- and CD106 (VCAM-1)-dependent mechanism. *J Clin Invest*. 2001;107(3):305-315.
35. Hendriks RW, Yuvaraj S, Kil LP. Targeting Bruton's tyrosine kinase in B cell malignancies. *Nat Rev Cancer*. 2014;14(4):219-232.

36. Hoellenriegel J, Meadows SA, Sivina M, et al. The phosphoinositide 3'-kinase delta inhibitor, CAL-101, inhibits B-cell receptor signaling and chemokine networks in chronic lymphocytic leukemia. *Blood*. 2011;118(13):3603-3612.
37. Linley A, Krysov S, Ponzoni M, Johnson PW, Packham G, Stevenson FK. Lectin binding to surface Ig variable regions provides a universal persistent activating signal for follicular lymphoma cells. *Blood*. 2015;126(16):1902-1910.
38. Buchner M, Baer C, Prinz G, et al. Spleen tyrosine kinase inhibition prevents chemokine- and integrin-mediated stromal protective effects in chronic lymphocytic leukemia. *Blood*. 2010;115(22):4497-4506.
39. Victora GD, Nussenzweig MC. Germinal centers. *Annu Rev Immunol*. 2012;30:429-457.
40. Chang KC, Huang X, Medeiros LJ, Jones D. Germinal centre-like versus undifferentiated stromal immunophenotypes in follicular lymphoma. *J Pathol*. 2003;201(3):404-412.
41. Jarjour M, Jorquera A, Mondor I, et al. Fate mapping reveals origin and dynamics of lymph node follicular dendritic cells. *J Exp Med*. 2014;211(6):1109-1122.
42. Bannard O, Horton RM, Allen CD, An J, Nagasawa T, Cyster JG. Germinal center centroblasts transition to a centrocyte phenotype according to a timed program and depend on the dark zone for effective selection. *Immunity*. 2013;39(5):912-924.
43. Cremasco V, Woodruff MC, Onder L, et al. B cell homeostasis and follicle confines are governed by fibroblastic reticular cells. *Nat Immunol*. 2014;15(10):973-981.
44. Yang CY, Vogt TK, Favre S, et al. Trapping of naive lymphocytes triggers rapid growth and remodeling of the fibroblast network in reactive murine lymph nodes. *Proc Natl Acad Sci U S A*. 2014;111(1):E109-118.
45. Endres R, Alimzhanov MB, Plitz T, et al. Mature follicular dendritic cell networks depend on expression of lymphotoxin beta receptor by radioresistant stromal cells and of lymphotoxin beta and tumor necrosis factor by B cells. *J Exp Med*. 1999;189(1):159-168.
46. Tokoyoda K, Hauser AE, Nakayama T, Radbruch A. Organization of immunological memory by bone marrow stroma. *Nat Rev Immunol*. 2010;10(3):193-200.
47. Anthony BA, Link DC. Regulation of hematopoietic stem cells by bone marrow stromal cells. *Trends Immunol*. 2014;35(1):32-37.
48. Dubey LK, Lebon L, Mosconi I, et al. Lymphotoxin-Dependent B Cell-FRC Crosstalk Promotes De Novo Follicle Formation and Antibody Production following Intestinal Helminth Infection. *Cell Rep*. 2016;15(7):1527-1541.
49. Barone F, Nayar S, Campos J, et al. IL-22 regulates lymphoid chemokine production and assembly of tertiary lymphoid organs. *Proc Natl Acad Sci U S A*. 2015;112(35):11024-11029.
50. Fleige H, Ravens S, Moschovakis GL, et al. IL-17-induced CXCL12 recruits B cells and induces follicle formation in BALT in the absence of differentiated FDCs. *J Exp Med*. 2014;211(4):643-651.
51. Yang ZZ, Novak AJ, Ziesmer SC, Witzig TE, Ansell SM. Malignant B cells skew the balance of regulatory T cells and TH17 cells in B-cell non-Hodgkin's lymphoma. *Cancer Res*. 2009;69(13):5522-5530.
52. Mraz M, Zent CS, Church AK, et al. Bone marrow stromal cells protect lymphoma B-cells from rituximab-induced apoptosis and targeting integrin alpha-4-

beta-1 (VLA-4) with natalizumab can overcome this resistance. *Br J Haematol*. 2011;155(1):53-64.
53. Rajnai H, Bodor C, Balogh Z, et al. Impact of the reactive microenvironment on the bone marrow involvement of follicular lymphoma. *Histopathology*. 2012;60(6B):E66-75.
54. Krumbholz M, Theil D, Cepok S, et al. Chemokines in multiple sclerosis: CXCL12 and CXCL13 up-regulation is differentially linked to CNS immune cell recruitment. *Brain*. 2006;129(Pt 1):200-211.
55. Madge LA, May MJ. Classical NF-kappaB activation negatively regulates noncanonical NF-kappaB-dependent CXCL12 expression. *J Biol Chem*. 2010;285(49):38069-38077.
56. Zhang Q, Guo R, Schwarz EM, Boyce BF, Xing L. TNF inhibits production of stromal cell-derived factor 1 by bone stromal cells and increases osteoclast precursor mobilization from bone marrow to peripheral blood. *Arthritis Res Ther*. 2008;10(2):R37.
57. Chen SS, Chang BY, Chang S, et al. BTK inhibition results in impaired CXCR4 chemokine receptor surface expression, signaling and function in chronic lymphocytic leukemia. *Leukemia*. 2016;30(4):833-843.
58. Beider K, Ribakovsky E, Abraham M, et al. Targeting the CD20 and CXCR4 pathways in non-hodgkin lymphoma with rituximab and high-affinity CXCR4 antagonist BKT140. *Clin Cancer Res*. 2013;19(13):3495-3507.
59. Feig C, Jones JO, Kraman M, et al. Targeting CXCL12 from FAP-expressing carcinoma-associated fibroblasts synergizes with anti-PD-L1 immunotherapy in pancreatic cancer. *Proc Natl Acad Sci U S A*. 2013;110(50):20212-20217.
60. Aguilar-Hernandez MM, Blunt MD, Dobson R, et al. IL-4 enhances expression and function of surface IgM in CLL cells. *Blood*. 2016;127(24):3015-3025.
61. Blunt MD, Koehrer S, Dobson R, et al. The dual Syk/JAK inhibitor cerdulatinib antagonises B-cell receptor and microenvironmental signaling in chronic lymphocytic leukemia. *Clin Cancer Res*. 2017.

FIGURE LEGENDS

Figure 1: Expression of CXCL12 within FL cell niches

(**A**) Tonsil and FL LN sections were stained with mouse IgG1 anti-CXCL12 and mouse IgM anti-CD21L antibodies followed by appropriate secondary antibodies. Dotted lines indicate normal and malignant follicles. Scale bar, 100µm. (**B**) *CXCL12* was quantified by QPCR in frozen tonsil (n=5) and FL-LN (n=12) sections. ****P*<0.001. (**C**) Sections from invaded FL BM were stained with mouse IgG1 anti-CXCL12 and rabbit anti-CD20 antibodies followed by appropriate secondary antibodies. Nuclei were counterstained with SytoxBlue (white). Dotted lines indicate the bone. Scale bar, 100µm. Boxes indicate the areas magnified in lower panels including intratumoral zone (left) and extratumoral zone (right panel) where scale bar represents 20µm. (**D**) CXCL12 concentration was measured by ELISA in BM plasma from healthy donors (HD, n=20) and FL patients (n=20). *****P*<0.0001. (**E**) *CXCL12* was quantified by QPCR in whole BM cells (left panel) and BM-MSCs (right panel) obtained from HD (n=5 and n=6; respectively) and FL patients (n=20 and n=9; respectively). **P*<0.05.

Figure 2: Characterization of stromal cell primed by TNF/LT *versus* IL-4

(**A**) *CXCL12* was quantified at RNA (QPCR, left panel) and protein (ELISA, right panel) levels in ADSCs treated by TNF/LT or IL-4 for 3 days. In QPCR experiments, an arbitrary value of 1 was assigned to untreated cells (UNT). Results represent the mean +/- SD from 7 experiments. **P*<0.05 (**B**) ADSCs were stimulated by TNF/LT, IL-4, or left untreated (UNT) for 3 days before quantification of *VCAM1, TGM2*, and *PDPN* expression by QPCR (n=7). The arbitrary value of 1 was assigned to UNT cells. In addition, VCAM-1/CD106 expression was evaluated by flow cytometry (n=5) and the ratio of mean fluorescence intensity (RMFI) was determined by comparison with an appropriate control isotype. **P*<0.05, ***P*<0.01. (**C**) ADSCs were cultured for 3 days with TNF/LT, IL-4, or left untreated (UNT) before fixation and transglutaminase and podoplanin staining. Nuclei were counterstained with SytoxBlue (white). Scale bars, 50µm. (**D**) ADSCs were co-cultured for 2 days with purified FL B cells expressing detectable (TNF^{hi}, n=6) or undetectable (TNF^{lo}, n=7) amounts of TNF as measured by ELISA, before sorting of $CD45^{neg}CD105^{pos}DAPI^{neg}$ viable stromal cells and *CXCL12* quantification by Q-PCR. The arbitrary value of 1

was assigned to ADSCs cultured alone (UNT). *P<0.05, **P<0.01 (**E**) ADSCs were co-cultured for 2 days with purified FL-T_{FH} before sorting of $CD45^{neg}CD105^{pos}DAPI^{neg}$ viable stromal cells and *CXCL12* quantification by Q-PCR. Results represent the mean +/- SD from 4 experiments. *P<0.05.

Figure 3: Expression and function of IL-4 within FL cell niches

(**A**) *IL4* was quantified by QPCR in frozen tonsil (n=5) and FL-LN (n=12) sections. *P<0.05. (**B**) *IL4* was quantified by QPCR in whole BM cells from HD (n=5) and FL patients (n=20). ****P<0.0001. (**C**) Immunohistochemical staining for CXCL12 and pSTAT6 on reactive tonsil (a-b), FL LN with high CXCL12/pSTAT6 expression (c-d) and FL LN with low CXCL12/pSTAT6 expression (e-f), Original magnification: x100 (a-b, scale bars, 100 μm), x200 (c-f, scale bars, 50 μm). (**D**) Semi-quantitative assessment of CXCL12 and pSTAT6 on FL tissue biopsies arranged on TMA. CXCL12 was scored positive when the expression was higher than in reactive GC and pSTAT6 was scored positive considered positive when frequent nuclear positive cells within the malignant follicles were observed. (**E**) Correlation between *IL4* and *CXCL12* expression across the 20 FL BM samples.

Figure 4: Impact of IL-4 on stromal cells committed to lymphoid stroma

(**A-B**) ADSCs were primed or not for 3 days with TNF/LT before treatment with TNF/LT, IL-4, or nothing (UNT) for 3 additional days and quantification of *CXCL12*, *TGM2* and *VCAM1* by QPCR. The arbitrary value of 1 was assigned to ADSC maintained without any cytokine during all the 6-day experiment. In addition, CXCL12 concentration was assessed by ELISA. Results represent the mean +/- SD from 6 to 7 experiments. *P<0.05. (**C**) ADSCs were primed or not for 24h with TNF/LT, starved for 2h, and then treated with IL4 for 5 minutes. STAT6 activation was first evaluated by flow cytometry (left panel) and quantified as the ratio of mean fluorescence intensity (RMFI) of PSTAT6 staining in IL-4 treated *versus* IL-4 untreated cells (n=6). In addition, STAT6, pSTAT6 and β-actin expression was determined by western blot and one representative experiment out of 2 is shown. *P<0.05, ns: not significant.

Figure 5: IL-4/CXCL12 loop in a model of inducible ectopic lymphoid organ in mice

(**A**) Quantitative RT-PCR analysis of mRNA transcript for *Il4* in WT mice on days 0, 5, 8, 15, and 23 post cannulation (p.c.), normalized to *Pdgfrβ*. Relative expression was calibrated to 0 p.c. salivary glands. **P*<0.05; ***P*<0.01 versus day 0. Results represent two experiments with four to six glands analyzed per group. (**B**) Quantitative RT-PCR analysis of mRNA transcript for *Cxcl12* in WT mice, *Il4*-/- mice, and *Il4r*-/- mice on days 0, 5, 8, 15, and 23 post cannulation (p.c.), normalized to *Pdgfrβ.* Relative expression was calibrated to 0 p.c. salivary glands. **P*<0.05; ***P*<0.01 versus day 0. Results represent two experiments with four to six glands analyzed per group and are represented as the mean +/- SD. Relative expression was calibrated to 0 p.c. salivary glands. **P*<0.05; ***P*<0.01.

Figure 6: CXCL12 signaling and functional impact on FL B cells

(**A**) Primary FL B cells pretreated or not with the CXCR4 antagonist AMD3100 or the Btk inhibitor Ibrutinib or PI3K-δ inhibitor Idelalisib were subjected to chemotaxis assay in response to CXCL12. Results are presented as the mean +/- SD of the migration index (n=6). **P*<0.05. (**B**) Primary FL B cells were labeled with CFSE, treated or not with AMD3100, and incubated for 2h on either CXCL12-Fc coated wells (left panel) or ADSC confluent cell monolayer (right panel). ADSCs have been transduced 48h before by CXCL12 targeting siRNA or control (Ctrl) siRNA. Adhesion percentage was calculated by comparing the residual fluorescence after adhesion with the fluorescence of the input. Shown is one representative experiment out of 2 (left) or mean +/- SD from 6 experiments (right). **P*<0.05. (**C**) Primary FL-B cells were starved for 4h and stimulated with uncoated (Ctrl) or CXCL12 Fc-coated beads for 60min. Western Blot revealed pSyk, Syk, pErk, Erk, and β-actin. Results are presented as the mean +/- SD from 3 experiments and one representative experiment is shown. (**D**) Primary FL B cells were starved for 4h, and pretreated or not by Ibrutinib before stimulation with uncoated or CXCL12 Fc-coated beads for 60min and quantification of pErk, Erk, and β-actin by western blot. Results are presented as the mean +/- SD from 4 experiments and one representative experiment is shown.

Figure 1

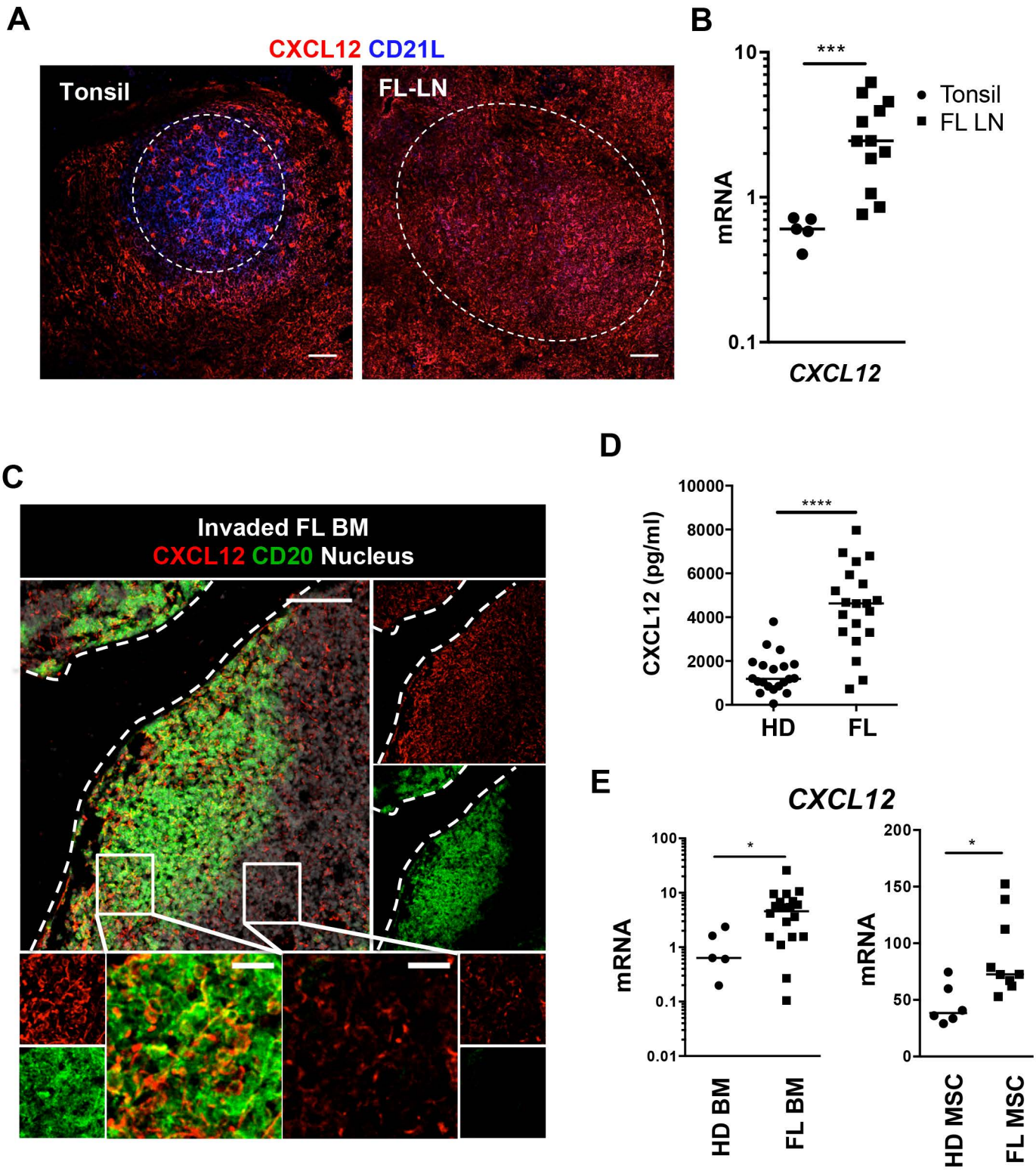

A
CXCL12 CD21L
Tonsil
FL-LN
B
***
Tonsil
FL LN
mRNA
10
1
0.1
CXCL12
C
Invaded FL BM
CXCL12 CD20 Nucleus
D
****
CXCL12 (pg/ml)
10000
8000
6000
4000
2000
0
HD
FL
E
CXCL12
*
mRNA
100
10
1
0.1
0.01
HD BM
FL BM
*
mRNA
200
150
100
50
0
HD MSC
FL MSC

Figure 2

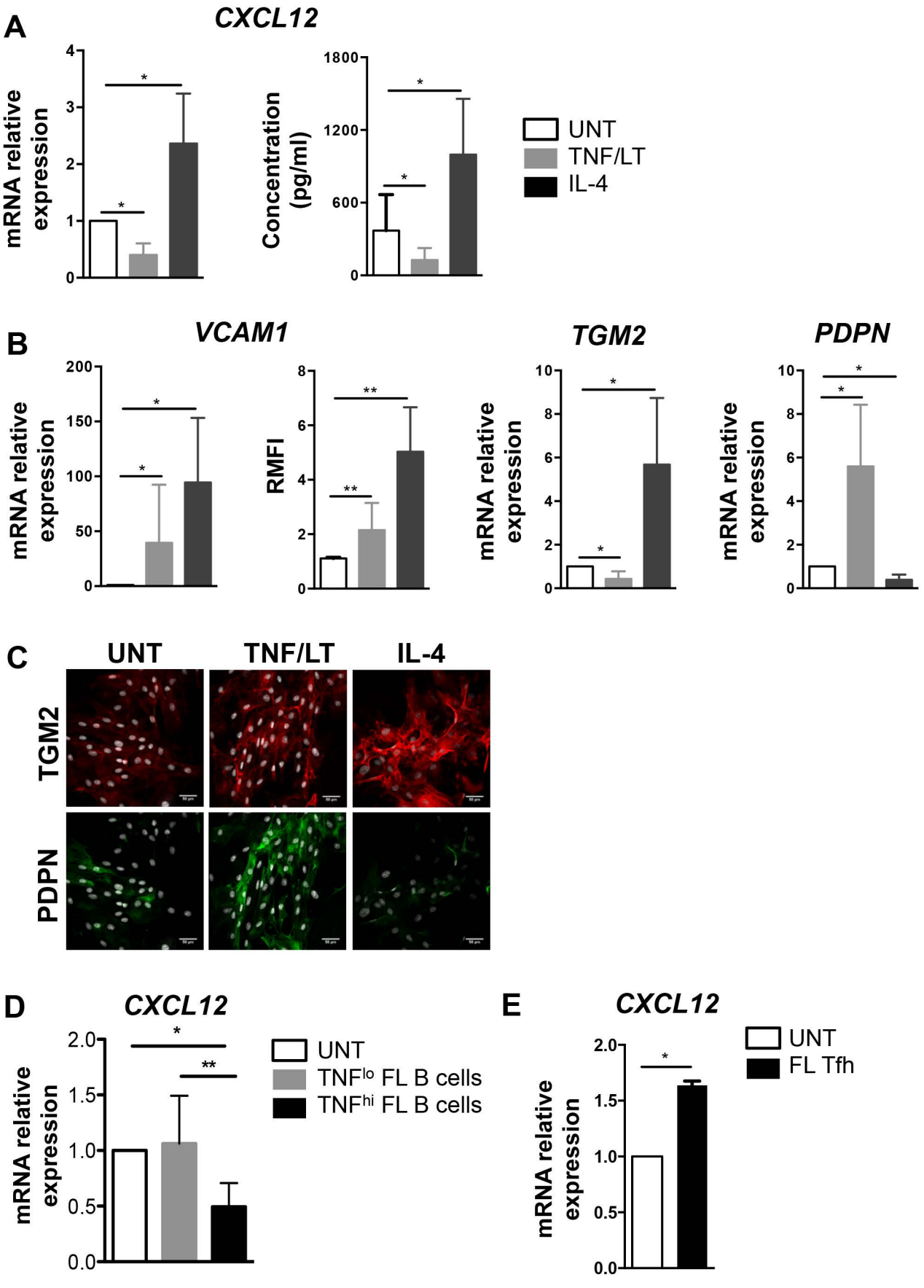

A
CXCL12
mRNA relative expression
Concentration (pg/ml)
UNT
TNF/LT
IL-4
B
VCAM1
TGM2
PDPN
mRNA relative expression
RMFI
C
UNT
TNF/LT
IL-4
TGM2
PDPN
D
CXCL12
mRNA relative expression
UNT
TNFlo FL B cells
TNFhi FL B cells
E
CXCL12
mRNA relative expression
UNT
FL Tfh

Figure 3

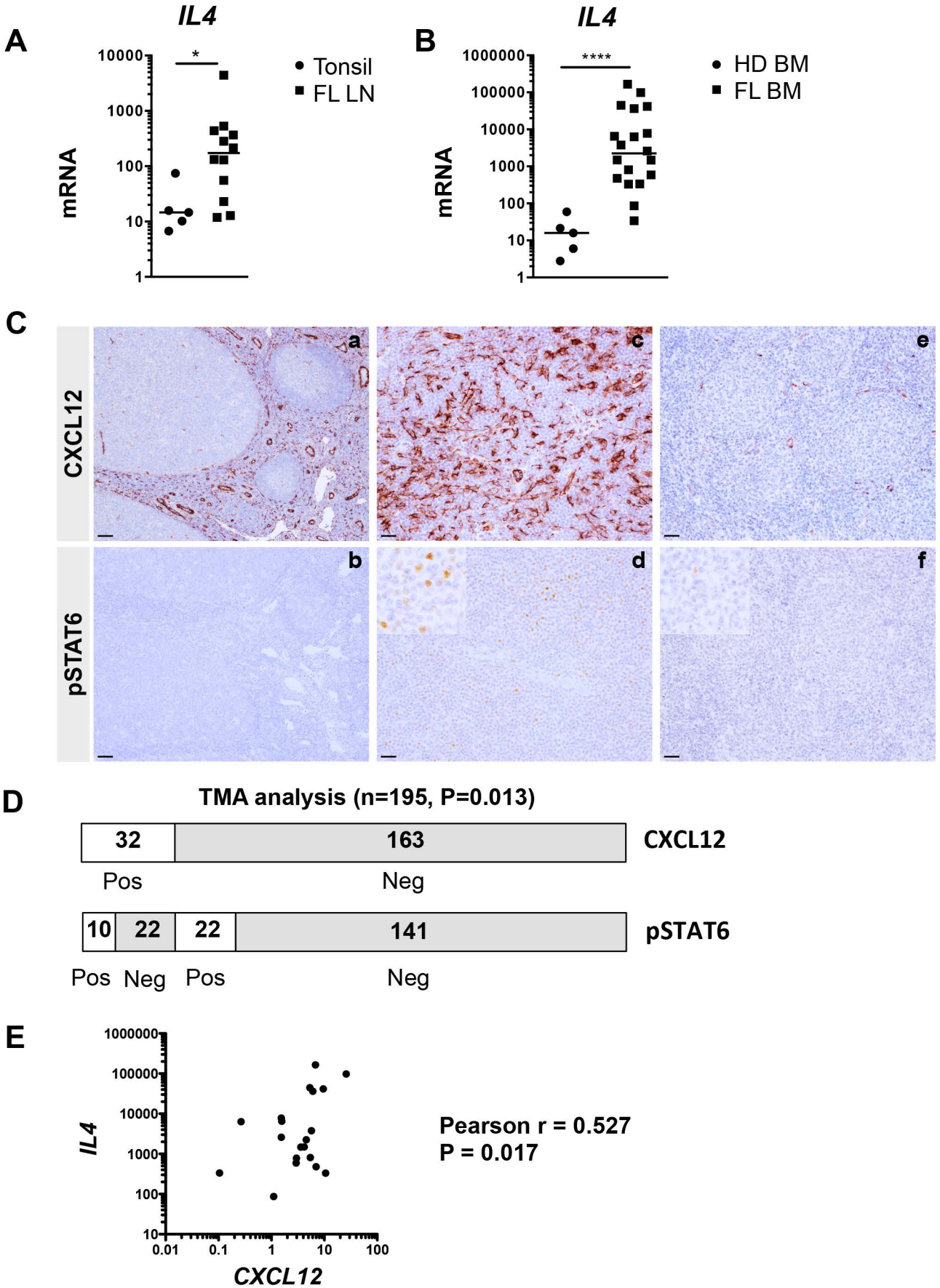

A
IL4
mRNA
10000
1000
100
10
1
*
Tonsil
FL LN
B
IL4
mRNA
1000000
100000
10000
1000
100
10
1
****
HD BM
FL BM
C
CXCL12
pSTAT6
a
b
c
d
e
f
D
TMA analysis (n=195, P=0.013)
32
163
CXCL12
Pos
Neg
10
22
22
141
pSTAT6
Pos
Neg
Pos
Neg
E
IL4
1000000
100000
10000
1000
100
10
0.01
0.1
1
10
100
CXCL12
Pearson r = 0.527
P = 0.017

Figure 4

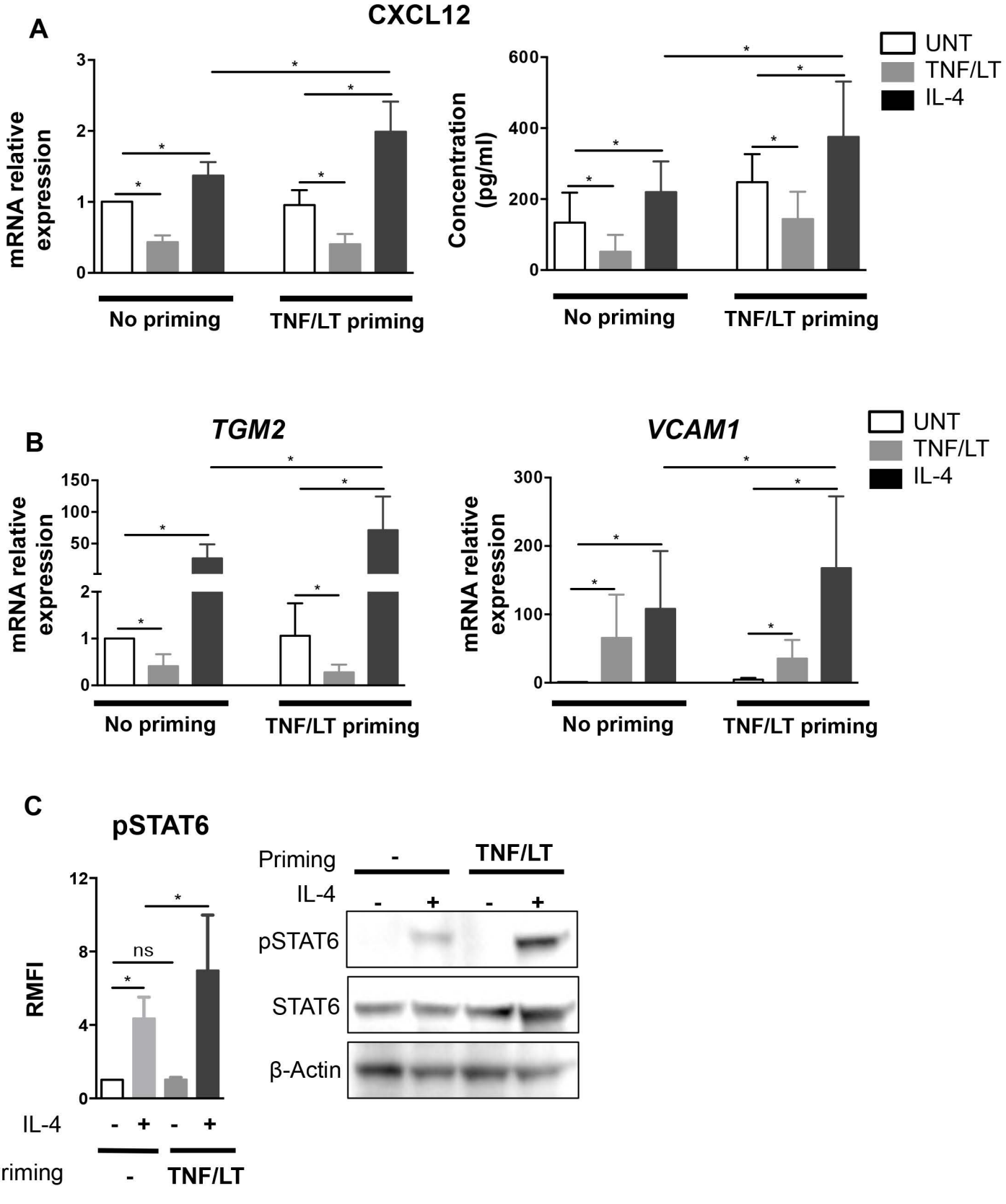

A
CXCL12
mRNA relative expression
Concentration (pg/ml)
UNT
TNF/LT
IL-4
No priming
TNF/LT priming
B
TGM2
VCAM1
mRNA relative expression
UNT
TNF/LT
IL-4
No priming
TNF/LT priming
C
pSTAT6
RMFI
ns
IL-4
Priming
-
TNF/LT
pSTAT6
STAT6
β-Actin

Figure 5

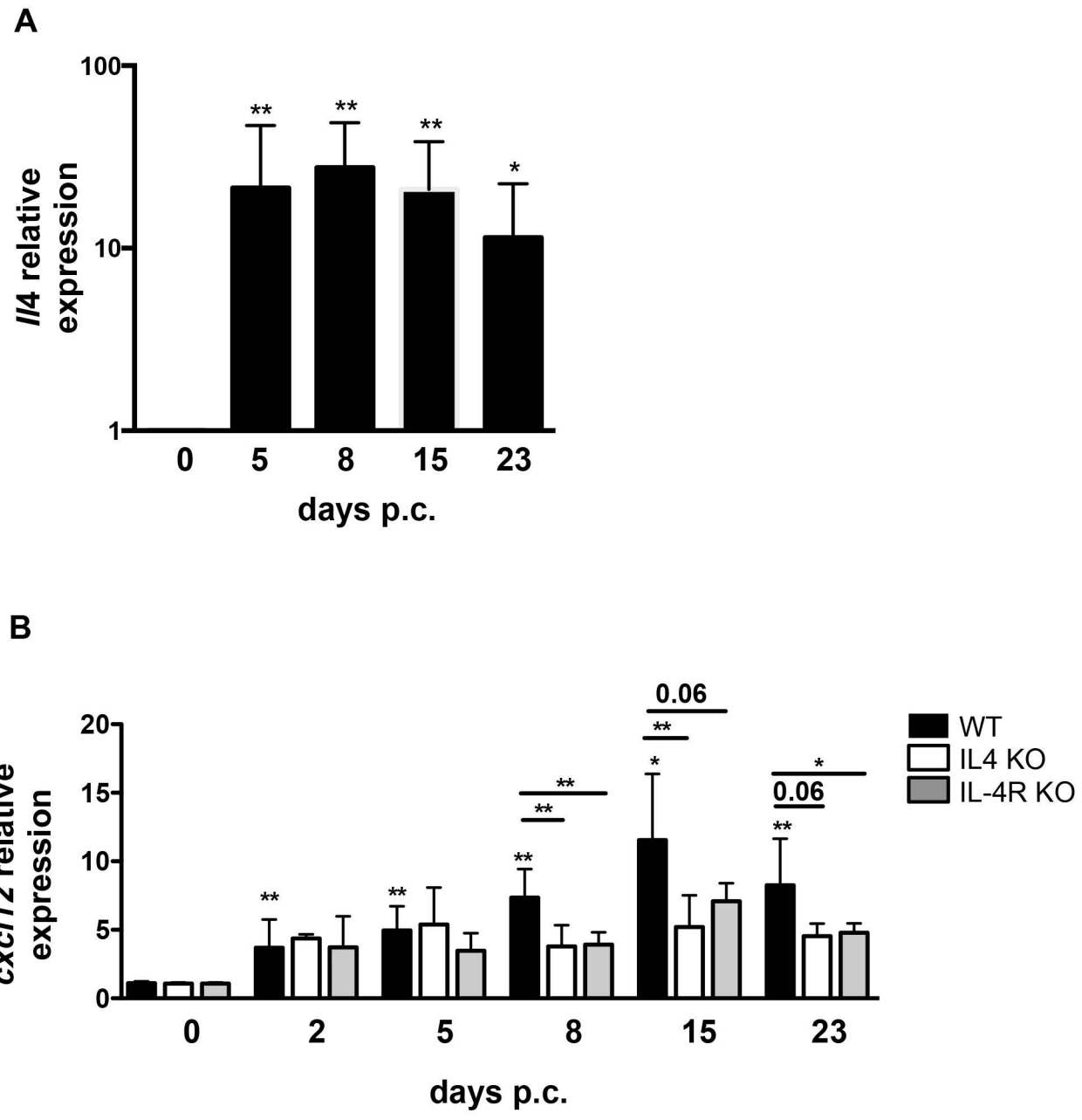
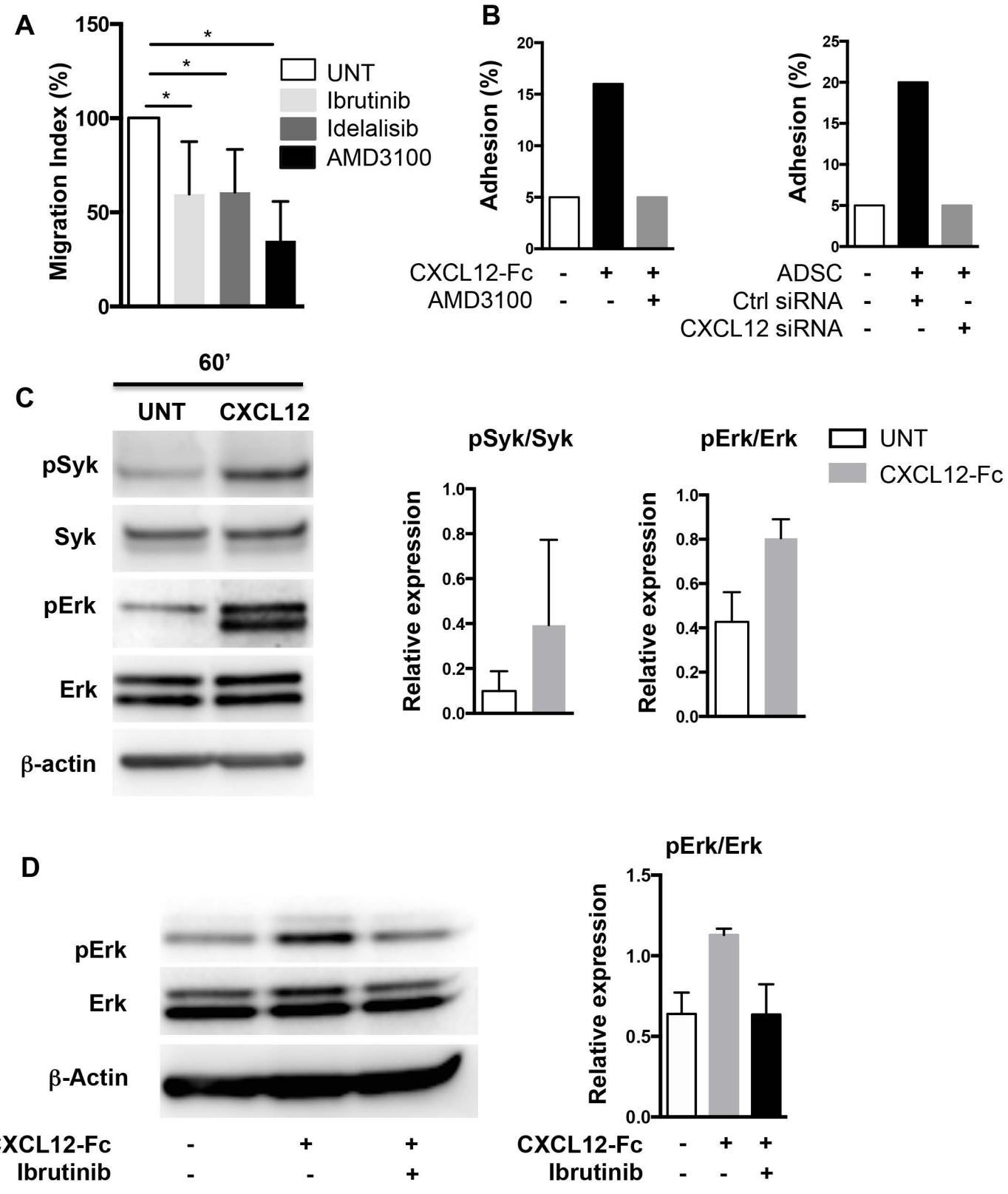

A
100
10
1
Il4 relative expression
**
**
**
*
0
5
8
15
23
days p.c.
B
20
15
10
5
0
cxcl12 relative expression
0.06
0.06
WT
IL4 KO
IL-4R KO
0
2
5
8
15
23
days p.c.

Figure 6


A
Migration Index (%)
150
100
50
0
*
*
*
UNT
Ibrutinib
Idelalisib
AMD3100
B
Adhesion (%)
20
15
10
5
0
CXCL12-Fc - + +
AMD3100 - - +
Adhesion (%)
25
20
15
10
5
0
ADSC - + +
Ctrl siRNA - + -
CXCL12 siRNA - - +
C
60'
UNT
CXCL12
pSyk
Syk
pErk
Erk
β-actin
pSyk/Syk
Relative expression
1.0
0.8
0.6
0.4
0.2
0.0
pErk/Erk
Relative expression
1.0
0.8
0.6
0.4
0.2
0.0
UNT
CXCL12-Fc
D
pErk
Erk
β-Actin
CXCL12-Fc - + +
Ibrutinib - - +
pErk/Erk
Relative expression
1.5
1.0
0.5
0.0
CXCL12-Fc - + +
Ibrutinib - - +